

# RSC Advances



This is an *Accepted Manuscript*, which has been through the Royal Society of Chemistry peer review process and has been accepted for publication.

*Accepted Manuscripts* are published online shortly after acceptance, before technical editing, formatting and proof reading. Using this free service, authors can make their results available to the community, in citable form, before we publish the edited article. This *Accepted Manuscript* will be replaced by the edited, formatted and paginated article as soon as this is available.

You can find more information about *Accepted Manuscripts* in the [Information for Authors](#).

Please note that technical editing may introduce minor changes to the text and/or graphics, which may alter content. The journal's standard [Terms & Conditions](#) and the [Ethical guidelines](#) still apply. In no event shall the Royal Society of Chemistry be held responsible for any errors or omissions in this *Accepted Manuscript* or any consequences arising from the use of any information it contains.

## ARTICLE

## Reducing Graphene Oxide with Modified Birch Reaction

Cite this: DOI: 10.1039/x0xx00000x

Jien Yang<sup>b</sup>, Yilei Wang<sup>a</sup>, Jing Wang<sup>a</sup>, Mary B. Chan-Park<sup>\*a</sup>

Received 00th January 2014,  
Accepted 00th January 2012

DOI: 10.1039/x0xx00000x

www.rsc.org/

An effective and facile method have been developed to reduce graphene oxide (GO) in alkyl amine solution using alkali metal as reducing agent. The alkali metal donates electrons to the GO and the oxygen-containing functional groups were eliminated to produce high-quality reduced graphene oxide (RGO).

### Introduction

Finding an economical method to produce high-quality graphene sheets in large-scale has drawn great attention of many scientists in various disciplines since the discovery of graphene by Geim and Novoselov in 2004<sup>1</sup>. Various methods have been developed to produce high-quality graphene<sup>2, 3</sup>, such as chemical vapor deposition<sup>4</sup>, epitaxial growth<sup>5</sup>, micromechanical exfoliation<sup>6</sup>, and exfoliation of graphite in solvents<sup>7-9</sup>. Reduction of graphene oxide (GO) to reduced graphene oxide (RGO) is a useful approach<sup>10-12</sup> and we report herein a simple, effective and scalable reduction method.

Chemical or thermal reduction of graphene oxide could eliminate inserted-functional groups and partially recover the intrinsic conjugated structure of graphene. Many reducing agents have been adopted to produce RGO from GO, including hydrazine<sup>13</sup>, alcohol<sup>14</sup>, sodium borohydride<sup>15</sup>, ascorbic acid<sup>16</sup>, and metal powder<sup>17</sup>. These reagents in various solutions have been reported to give a high degree recovery of conjugated structure of RGO. While the reduction process can substantially restore the structure of graphene by eliminating oxygen-containing groups in GO, the oxidation of graphite disrupts the sp<sup>2</sup> delocalized electron structure, leading to sp<sup>3</sup> carbons in GO and leaving a significant number of defects<sup>18</sup>. A high degree of restoration of the graphene  $\pi$ -conjugated structure in RGO and the elimination of impurities are essential for production of high quality graphene-based materials with superior properties, particularly conductivity, in large-scale.

Birch reaction entails the use of liquid ammonia and sodium (or lithium or potassium) and an alcohol. In the historical evolution of the Birch reaction, low molecular weight amines and ethylenediamine have been used to replace the original liquid ammonia as reaction solvent and to assist the addition of solvated electrons to the aromatic rings<sup>19</sup>. There is a reported application of a similar modified Birch reaction in synthetic organic chemistry to convert oxiranes to olefins with deoxygenation<sup>20</sup>. With this in mind, we have investigated the

reduction of GO in tris(2-aminoethyl) amine and with sodium and found the reaction to be very effective. This paper reports the solution-based reduction of GO through a modified Birch Reaction using alkali metal in alkylamine as the reducing solution. The effectiveness of this facile method for production of RGO was investigated with various analytical tools, such as X-ray photoemission spectroscopy (XPS), X-ray diffraction (XRD), Thermo-gravimetric analyses (TGA) and Fourier transform infrared spectroscopy (FT-IR). The reduction process dramatically reduces the sheet resistance (SR), from  $3 \times 10^4 \Omega \square$  for GO to  $30 \Omega \square$  for as-prepared RGO. The SR of RGO declines further, to as low as  $3.0 \Omega \square$ , after annealing at 1000°C for 5 min. This reduction method dramatically improves the electrical conductivity of RGO, promoting progress toward application of RGO in various fields.

### Results and Discussion

Graphene oxide used in this paper was fabricated according to a previously reported procedure<sup>21</sup>. The GO was reduced via a modified Birch reduction reaction with a strong electron donor (sodium) in Tris(2-aminoethyl) amine.

The three XRD patterns in Fig. 1A (pristine graphite, GO and RGO) clearly indicate changes in interlayer distance produced by the successive processing steps. GO displays a relatively large distance of 0.875 nm ( $2\theta=10.103^\circ$ ) owing to the addition of hydroxyl, epoxy, and carbonyl functional groups to the planar backbone during the chemical oxidation. The interlayer distance of RGO is reduced considerably to about 0.379 nm, near to that of pristine graphite (0.334 nm), which is consistent with a highly reduced product<sup>22</sup>. The broadened XRD peak of RGO suggests the presence of residual amine within the interlamellar spaces of the reduced graphene oxide<sup>23</sup>.

Fourier transform infrared spectroscopy (FTIR presented in Figure 1B) indicates changes in functional groups in graphite, GO and RGO. The peaks at 3443 and 1635 cm<sup>-1</sup>, present in all the FTIR

spectra, correspond to hydroxyl stretching and vibration modes from the moisture absorbed on the samples<sup>24</sup>. The strong broad peaks at 3443  $\text{cm}^{-1}$  are also due to the superposition of the vibration of hydroxyl groups that arise in graphite oxidation. The small, narrow peaks at 2919 and 2849  $\text{cm}^{-1}$  are due to C-H bonds on graphene sheet edges. The long-wavelength portion of the GO spectrum is complex and contains several features which are much stronger in GO than (if present at all) in the graphite and RGO spectra. These include peaks at 1728  $\text{cm}^{-1}$  due to the stretching vibration of C=O in carbonyl and carboxylic acid groups, the C-O stretching vibration of carboxyl group at 1407  $\text{cm}^{-1}$  and C-O bond vibrations of epoxy and alkoxy at 1202 and 1076  $\text{cm}^{-1}$  respectively. These changes confirm successful insertion of oxygen-containing groups in the processing of graphite to GO and their subsequent removal in the reduction procedure. New peaks in the RGO spectrum at 1566 and 1202  $\text{cm}^{-1}$  (marked with \*) are attributable to the N-C stretching vibration<sup>25</sup>, indicating residual amine molecules on the planar structure. The peak at 579  $\text{cm}^{-1}$  is due to a residue of sodium ethylate.

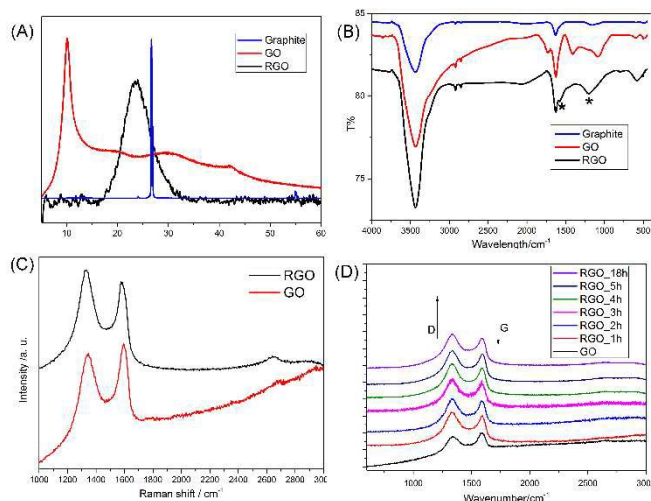


**Fig. 1** (A) XRD patterns, (B) FTIR spectra, (C) Raman spectra of pristine graphite, graphene oxide (GO) and reduced graphene oxide (RGO) respectively (there are only GO and RGO in C), (D) Time-resolved Raman spectroscopy during reduction.

Figure 1C shows the micro-Raman spectra of GO and RGO. The GO spectrum exhibits a D band at 1344  $\text{cm}^{-1}$  arising from structural defects created by the attachment of oxygen-containing functional groups on graphite. It is due to K-point phonons with a breathing model of  $A_{1g}$  symmetry, suggesting the decrease of  $\text{sp}^2$  domains of the graphene sheets, possibly due to a high degree of oxidation<sup>26, 27</sup>. GO also has a G band at about 1597  $\text{cm}^{-1}$  due to  $\text{sp}^2$  carbon atoms resonance at higher frequencies, attributed to the first-order scattering of the  $E_{2g}$  mode<sup>28</sup>. There is a small overtone 2D band at 2696  $\text{cm}^{-1}$ . The intensity of 2D band in RGO increased prominently and shifted to 2649  $\text{cm}^{-1}$  after the reduction processing, confirming successful restoration of graphene conjugated structure<sup>29</sup>.

From Fig. 1C, the value of D/G ( $I_D/I_G$ ) was 1.19 in GO, increasing to 1.96 after reduction for 3h with sodium in alkali solution. Time-dependent Raman spectroscopy (Fig. 1D) was also used to monitor the process of reduction. The areal density of unrepaired defects created in the course of removal of oxygen-containing functional groups increases with extension of the reaction time. As a result, the

value of  $I_D/I_G$  increased during the procedure and subsequently decreased slightly, which is attributed to formation of the  $\text{sp}^2$  carbon atoms during reduction processing<sup>30</sup>. The Raman spectral data corroborates that sodium in alkali solution successful reduce GO to RGO.

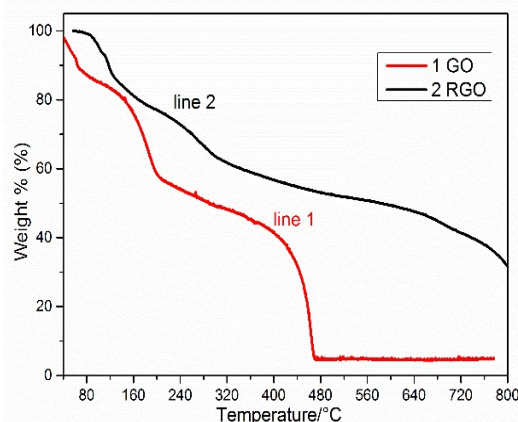


**Fig.2** TGA curves of GO and as-prepared RGO.

Thermogravimetric analysis (TGA, Fig. 2) was used to investigate the thermal behaviour of GO and RGO. The weight profiles of powder samples were measured under  $\text{N}_2$  flow. The weight loss of GO up to 100°C, ~15wt%, is attributable primarily to the evaporation of water trapped in the samples. The changes of RGO to this temperature (~5wt%) was lower than that of GO, indicating less water absorbed on RGO than on GO. While GO showed weight loss of about 27wt% from 100°C to 201°C, due to a combination of moisture evaporation and removal of unstable functional groups produced during oxidation, RGO lost less weight (~18wt%) in the same temperature range due to further water evaporation and removal of residual alkali molecules. There is dramatic GO weight loss above 400°C to 470°C, a consequence of carbon oxidation by trace oxygen in the  $\text{N}_2$  flow. RGO has a gradual weight loss from 300°C to 800°C. The lower and more gradual weight loss of RGO than of GO is evidence that GO has been reduced to RGO, because the graphene sheet is more stable than GO under thermal treatment.

The elemental composition and the quality of the GO, RGO, and annealed RGO were studied with XPS. Fig. 3 shows the wide-scan and  $\text{C}_{1s}$  high-resolution XPS spectra of the three materials. The oxygen content of RGO was much less than that of GO, confirming successful reduction. The  $\text{C}_{1s}$  peak of GO can be decomposed into 5 peaks as shown in Fig. 3B. The binding energies of the various carbon atoms in the samples were distinguishable<sup>27</sup>.

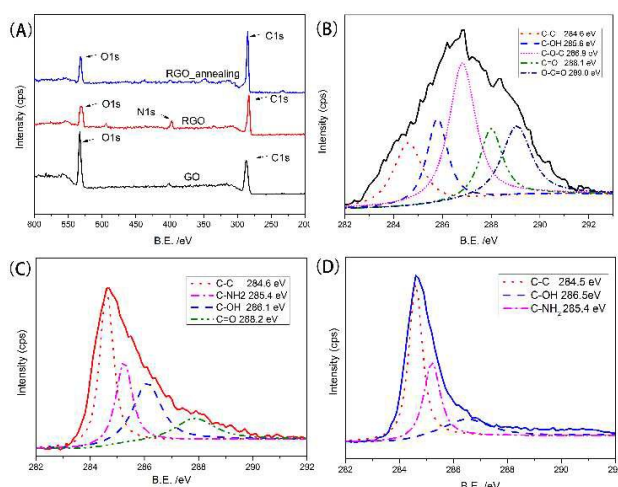
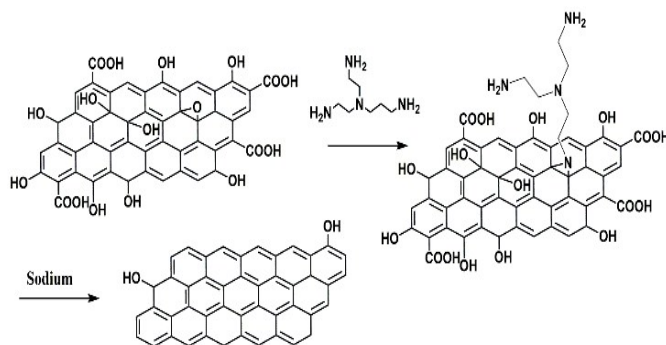


**Fig.3** XPS analyses of C1s peaks of GO, RGO and annealed RGO. (A) Survey scans. (B)-(D) High resolution scans with deconvolutions of the C1s peak of GO (B), RGO (C) and annealed RGO (D).

The GO peak C<sub>1s</sub> peak decomposition is O-C=O (289.0 eV), C=O (288.1 eV), C-O-C (286.9 eV), C-OH (285.6 eV) and C=C (284.6 eV). After reduction, the intensity of all the C<sub>1s</sub> peaks of hydroxyl, carbonyl and carboxyl carbon atoms, excepting C-OH, decreased dramatically compared to GO. RGO also has a new type of carbon, C-NH<sub>2</sub>, which is the residual of tris(2-aminethyl) amine in the sample. Annealing of the RGO in inert atmosphere resulted in further removal of functional groups. The high-quality of RGO from reduction may be judged by the elemental composition changes during the processing. It is apparent from inspection of Fig. 3A than the C/O ratio significantly increases from GO to RGO to annealed RGO; this visual impression is confirmed by the integrated peak areas of C1s and O1s in the respective samples. The C/O ratio increased from 0.84 in GO to 3.36 after the reduction with sodium in alkali solution and even further to 6.0 after sample annealing in argon atmosphere. We conclude that the most of the inserted functional groups in GO were eliminated in annealed RGO.<sup>30</sup>

The samples' O1s were also investigated in the high resolution XPS spectra (Fig. S2). There were significant changes in the O1s peak before and after the reduction, especially after the thermal treatment. There are three types of oxygen (C-O, C=O, O=C-OH) in O1s peak of GO; these correspond to three distinct oxygen-containing functional groups. The treatment with sodium in solution eliminated the C=O component completely and greatly decreased the other two types of oxygen (Fig. S2A). After annealing, only the C-OH peak remained. These results are identical to those measured with the C1s peaks. Nitrogen was also almost completely removed by annealing of the RGO samples. These results support the conclusion that reduction and annealing substantially recover the graphene structure.



**Scheme 1** The proposed reduction mechanism.

We infer a reduction mechanism of GO as shown in Scheme 1. The alkylamine could attach on the epoxide to form an imine on the basal structure of the graphene. With the assistance of alkylamine, the electron from sodium is transferred to the aromatic arene oxides or imines. This process is followed by departure of the corresponding metal oxide or amide and restoration of the C=C double bond. There are also some hydroxyl groups on the structure, consistent with the XPS spectra.

GO film fabricated by vacuum filtration has a huge sheet resistance, even would be insulator. After reduction and annealing, the RGO film's electrical conductivity was improved from 30k  $\Omega/\square$  to an average sheet resistance of 3.0 $\Omega/\square$  (supplementary information). The obtained RGO paper has high conductivity, because there is lower structural defect density<sup>31</sup> in the individual sheets and closer restacking of the RGO layers with reduction.

Figs. 4A-D show the morphology of annealed RGO film. After annealing, the film has a rougher surface and layered structure at the edges. The annealing also greatly improves the RGO film's electrical properties, consistent with what one would expect from the XPS spectra (Fig. 3 and Fig. S2). Residual traces of oxygen-containing functional groups and impurity would impair the electrical conductivity of RGO.

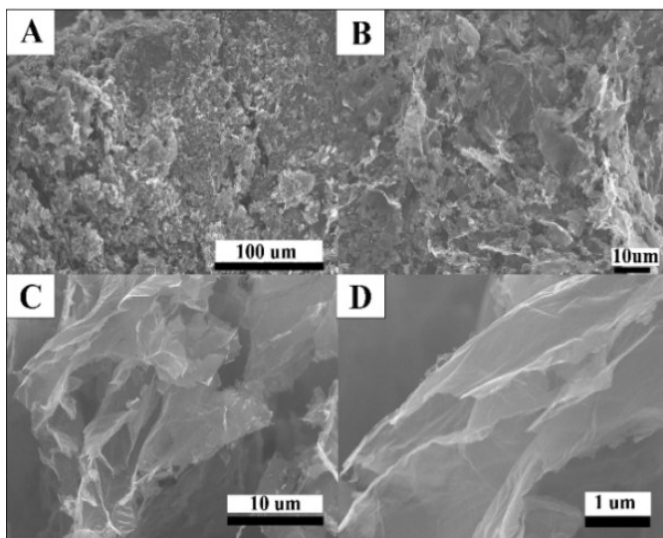


**Fig.4** SEM images of RGO film after annealing.

## Conclusions

We have developed a novel method to reduce GO in alkylamine solution with sodium as reducing agent. FTIR, Raman, XRD, TGA and XPS analyses confirm the successful reduction. The as-produced RGO exhibits high-quality, such as low sheet resistance and desirable nanoscale morphology. The excellent performance, simplicity and scalability of this method are progress toward application of RGO in various fields.

## Acknowledgements

This work was supported by an ASTAR grant (102 170 0141).

## Notes and references

<sup>a</sup> School of Chemical and Biomedical Engineering, Nanyang Technological University, 62 Nanyang Drive, Singapore 637459, Singapore. E-mail: mbechan@ntu.edu.sg

<sup>b</sup> Henan Key Laboratory of Photovoltaic Materials, Xinxiang 453007, P. R. China. E-mail: yjen@htu.cn.†

Electronic Supplementary Information (ESI) available: [Experiment section, FESEM of GO, Survey of O<sub>1s</sub> and electronic conductivity]. See DOI: 10.1039/b000000x/

1. K. S. Novoselov, A. K. Geim, S. V. Morozov, D. Jiang, Y. Zhang, S. V. Dubonos, I. V. Grigorieva and A. A. Firsov, *Science*, 2004, **306**, 666-669.
2. M. I. Katsnelson and A. Fasolino, *Acc. Chem. Res.*, 2013, **46**, 97-105.
3. Z. Z. Sun, D. K. James and J. M. Tour, *Journal of Physical Chemistry Letters*, 2011, **2**, 2425-2432.
4. I. N. Kholmanov, C. W. Magnuson, A. E. Aliev, H. Li, B. Zhang, J. W. Suk, L. L. Zhang, E. Peng, S. H. Mousavi, A. B. Khanikaev, R. Piner, G. Shvets and R. S. Ruoff, *Nano Lett.*, 2012, **12**, 5679-5683.
5. H. Huang, W. Chen, S. Chen and A. T. S. Wee, *ACS Nano*, 2008, **2**, 2513-2518.
6. Y. Zhang, J. P. Small, M. E. S. Amori and P. Kim, *Phys. Rev. Lett.*, 2005, **94**, 176803.
7. M. Cai, D. Thorpe, D. H. Adamson and H. C. Schniepp, *J. Mater. Chem.*, 2012, **22**, 24992-25002.
8. U. Khan, H. Porwal, A. O'Neill, K. Nawaz, P. May and J. N. Coleman, *Langmuir*, 2011, **27**, 9077-9082.
9. S. M. Notley, *Langmuir*, 2012, **28**, 14110-14113.
10. O. C. Compton and S. B. T. Nguyen, *Small*, 2010, **6**, 711-723.
11. D. C. Marcano, D. V. Kosynkin, J. M. Berlin, A. Sinitskii, Z. Z. Sun, A. Slesarev, L. B. Alemany, W. Lu and J. M. Tour, *ACS Nano*, 2010, **4**, 4806-4814.
12. J. Kim, L. J. Cote and J. Huang, *Acc. Chem. Res.*, 2012, **45**, 1356-1364.
13. S. Park, J. An, J. R. Potts, A. Velamakanni, S. Murali and R. S. Ruoff, *Carbon*, 2011, **49**, 3019-3023.
14. C.-Y. Su, Y. Xu, W. Zhang, J. Zhao, A. Liu, X. Tang, C.-H. Tsai, Y. Huang and L.-J. Li, *ACS Nano*, 2010, **4**, 5285-5292.
15. Y. Si and E. T. Samulski, *Nano Lett.*, 2008, **8**, 1679-1682.
16. J. Zhang, H. Yang, G. Shen, P. Cheng, J. Zhang and S. Guo, *Chem. Commun.*, 2010, **46**, 1112-1114.
17. Z. Fan, K. Wang, T. Wei, J. Yan, L. Song and B. Shao, *Carbon*, 2010, **48**, 1686-1689.
18. Y. Hernandez, V. Nicolosi, M. Lotya, F. M. Blighe, Z. Sun, S. De, I. T. McGovern, B. Holland, M. Byrne, Y. K. Gun'Ko, J. J. Boland, P. Niraj, G. Duesberg, S. Krishnamurthy, R. Goodhue, J. Hutchison, V. Scardaci, A. C. Ferrari and J. N. Coleman, *Nat Nano*, 2008, **3**, 563-568.
19. M. E. Garst, L. J. Dolby, S. Esfandiari, N. A. Fedoruk, N. C. Chamberlain and A. A. Avey, *J. Org. Chem.*, 2000, **65**, 7098-7104.
20. K. N. Gurudutt and B. Ravindranath, *Tetrahedron Lett.*, 1980, **21**, 1173-1174.
21. C. Bao, L. Song, W. Xing, B. Yuan, C. A. Wilkie, J. Huang, Y. Guo and Y. Hu, *J. Mater. Chem.*, 2012, **22**, 6088-6096.
22. E. Yoo, J. Kim, E. Hosono, H.-s. Zhou, T. Kudo and I. Honma, *Nano Lett.*, 2008, **8**, 2277-2282.
23. D. R. Dreyer, S. Murali, Y. Zhu, R. S. Ruoff and C. W. Bielawski, *J. Mater. Chem.*, 2011, **21**, 3443-3447.
24. X. Huang, N. Hu, R. Gao, Y. Yu, Y. Wang, Z. Yang, E. Siu-Wai Kong, H. Wei and Y. Zhang, *J. Mater. Chem.*, 2012, **22**, 22488-22495.
25. J.-I. Yan, G.-j. Chen, J. Cao, W. Yang, B.-h. Xie and M.-b. Yang, *New Carbon Mater.*, 2012, **27**, 370-376.
26. A. Ferrari and J. Robertson, *Phys. Rev. B*, 2000, **61**, 14095.
27. D. R. Dreyer, S. Park, C. W. Bielawski and R. S. Ruoff, *Chem. Soc. Rev.*, 2010, **39**, 228-240.
28. N. A. Kumar, S. Gambarelli, F. Duclairoir, G. Bidan and L. Dubois, *J. Mater. Chem. A*, 2013.
29. A. Ferrari, J. Meyer, V. Scardaci, C. Casiraghi, M. Lazzeri, F. Mauri, S. Piscanec, D. Jiang, K. Novoselov and S. Roth, *Phys. Rev. Lett.*, 2006, **97**, 187401.
30. I. K. Moon, J. Lee, R. S. Ruoff and H. Lee, *Nat. Commun.*, 2010, **1**, 73.
31. J. T. Robinson, F. K. Perkins, E. S. Snow, Z. Wei and P. E. Sheehan, *Nano Lett.*, 2008, **8**, 3137-3140.

Reduced graphene oxide was prepared in alkyl amine solution using alkali metal as reducing agent.

